Plasmonic refractive index sensor based on high birefrigent symmetrical photonic crystal fiber

YAZUSHA SHARMA[1, 2*], SHRUTI KALRA[2], RUKHSAR ZAFAR[1], RITAMBHARA[2]
[1]*Department of Electronics and Communication Engineering, Swami Keshvanand Institute of Technology, Management and Gramothan, Jaipur, India*
[2]*Department of Electronics and Communication Engineering, Jaipur Engineering College & Research Centre, Jaipur, India*

In the presented paper, we propose a sensing design of a photonic crystal fiber based on plasmonics finding its suitability to measure the variation in the refractive index of the analyte under consideration. The parameters such as sensitivity, reflectivity, confinement loss and birefringes play a vital role for a sensor suitable to measure various physical quantities in real life applications. The proposed sensor design is numerically investigated to analyze sensitivity, reflectivity, confinement loss and birefringes making it suitable for various sensing applications. The sensor exhibited high birefringes value 0.021401, which is recorded to be best for the sensitivity of a given sensor for the analytes depicting refractive index of 1.35. The higher values of birefringes accomplished with higher sensitivity and reduced values of nonlinearity makes the sensor suitable for numerous sensing applications. The design proposed can be easily fabricated making it cost effective along with ease of handling. The lowest confinement loss observed was 11.818 db/m. At refractive index of 1.4, this minimum loss making it suitable for sensing multifarious biological and chemical materials.

(Received September 29, 2022; accepted April 7, 2023)

Keywords: Plasmonics, Birefringes, Sensitivity, Confinement loss

1. Introduction

An outstanding control of sensing parameters of a sensor with the help of advanced technical and engineering based techniques has assisted and enhanced the suitability of photonic crystal fibers (PCF) for vast range of applications. PCFs are light guiding media designed with unique features, offering compact size, good adaptability, low loss; simple designing and excellent controlled guiding property, thus that resulting to magnify their potency as compared to the conventional optical fiber for enormous applications [1]. In addition to the aforesaid unique characteristics, PCF also have distinctive properties like high linearity [2], low losses [3], flat dispersion [3] and high birefringes [4] making them most demanding and choice of researchers and scientists for exploring their usage and applications in diversified fields. Recently PCFs have gained attention of many researchers due to their applications in plasmonics based sensing devices like water sensing [5], gas detection [5-6], chemical sensing [7] food quality testing [8], glucose level testing [8] etc. Many sensing applications are based on detection of change in refractive index of the substance under observation, further it is desirable that the sensor detects high sensitivity, and is capable of detecting very small and minute changes in the refractive index. Surface Plasmon resonance (SPR) based sensing methods are vastly adopted for numerous sensing applications as the phenomena used is capable of detecting minute changes in the refractive index of the material, which is one of the essential conditions for its application as a sensor [9-11].

Surface plasmonic resonance (SPR) phenomenon occurs when the frequency of the incident beam of light completely matches with the surface electron frequency, thus resulting to resonance condition and generation of strong surface Plasmon polariton (SPP) responsible for sensing applications [12,13]. SPR sensors mechanism offers ease to be incorporated with media like prism [3, 13], fiber grating [14], photonic crystal fiber [14] and others making them suitable sensing devices in various areas such as biomedical diagnosis [15,16], environmental monitoring [1,17], biochemical organic sample detection [18] etc. Plasmonics based PCF sensors are in great demand as they have overcome the problem of bulky size of prism based method and also offers high sensitivity and resolution as compared to optical fiber based sensing techniques [19]. PCF-SPR sensors offers suitability and ease of tailoring different parameters such as PCF diameter [20], pitch [21], plasmonics material thickness [20-22], modes of fiber [22], number of rings in cladding [23] and PCF lattice [23] and etc. The characteristics and performance of a SPR sensor can be easily controlled and altered with choice of suitable metal for phenomena of plasmonics generation. Significant number of sensors has widely used gold (Au) metal, as use of gold offers stability for larger wavelength range as compared to silver (Ag) [20, 22, 23]. Recent research papers portray effective use of thin oxide layers such as titanium oxides (TiO_2) [24], Indium Tin oxides (ITO) [23] along with metals (Au) and (Ag) to enhance the SPR effect [25]. There are several methods available such as extrusion, 3D printing, stack-and-draw, sol-gel casting, etc. for PCF fabrication. The

Stack-and-draw method is best choice for the fabrication of PCFs having multilayer and uniform circular air holes. It is believed that with the advancement of fabrication technologies theoretically demonstrated PCF-SPR sensor models will be produced cheaply for the identification of biochemical substances at a wide RI range [26-27].

In this paper we explore a simple PCF structure designed with two rings of air holes. The coating of metal films is situated to the outer portion of the PCF in lieu of internal portion as it increases its efficiency and reduces the fabrication complexity. Multilayer structure increase in fabrication complexity and tolerance still very demanding in the field of PCF based sensor as each layer has its own attributes. PCF-SPR sensors are classified into two categories. First, internally metal coated PCF structure where plasmonics material (metal) is selectively deposited inside the PCF and liquid analyte is selectively in filtered into air holes. So the number of layers can be minimized in this structure but in this technique the detection is very difficult to implement practically. Second, externally metal coated PCF where plasmonic materials are deposited on the outer surface of PCF. In this multilayer structure has more attention in research because of forward detection and ease of fabrication [27-28]. The different sensor parameters are calculated for different values of refractive index of analyte. The goal was to design and investigate a sensor based on simpler PCF design suitable to offer enhanced sensitivity, low losses and higher values of qualitative analysis.

2. Design and structure

The proposed design of the sensor is depicted in Fig. 1, designed with asymmetric solid core hexagonal lattice silica PCF consisting of two rings in the cladding region. The diameters of air holes in the two rings are selected in different orders and few air-holes are kept absent in the outermost ring of the cladding, in view for designing asymmetric PCF structure with suitable pitch (ʌ) as 2.3 μm. The cladding is surrounded with a four layer of different materials for the sensing phenomenon. The innermost layer is made of gold (Au), the most preferred plasmonic material for sensor of higher sensitivity. Gold was chosen in the proposed design, to overcome the challenges of oxidation of Ag with air. Gold has shown chemically inert property so the problem of oxidation can be minimized. Besides this, Gold is long term stable and easy to compatible with structure so it has a higher optical damping and has wide resonance wavelength peak that helps to enhance the sensitivity of the refractive index sensor [29-30].

The permittivity of gold is expressed as Eq. (1):

$$\varepsilon_m(\omega) = \varepsilon_\infty - \frac{\omega_p^2}{\omega(\omega+i\gamma)} \quad (1)$$

In above equation ε_∞ represents the relative permittivity for infinite frequency and is numerically stated as 3.7, γ = 2.73 10^{17} rad/sec depicts the collision frequency of electrons, ω_p = 1.38 10^{16} rad /sec represents the plasma frequency and ω denotes incident light angular frequency. The analyte layer is sandwiched between metal layer and titanium oxide (TiO_2) layer surrounding the cladding structure of the PCF based sensor. TiO_2 is being used as third layer as the combination of TiO_2 with gold shows the largest shift in resonance wavelength which help to improve the sensitivity of refractive index sensor. Due to shifting of resonance wave length, the other sensing parameters such as Q factor and figure of merit can be improved. Toluene is naturally occurring compound. It is a common component in gasoline, glues and other products. Toluene is a liquid that is colorless, water- insoluble and smells similar to paint thinners. Toluene occurs naturally occurred in crude oil at low levels [31, 32].

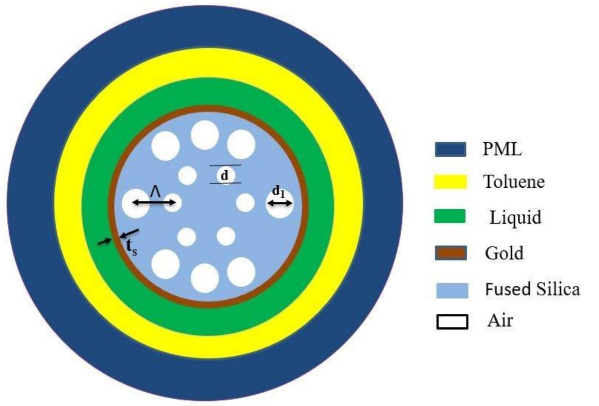

Fig. 1. Cross sectional view of the proposed hexagonal lattice PCF sensor with d=0.58μm, Λ=2.3 μm, d_1=0.78 μm (color online)

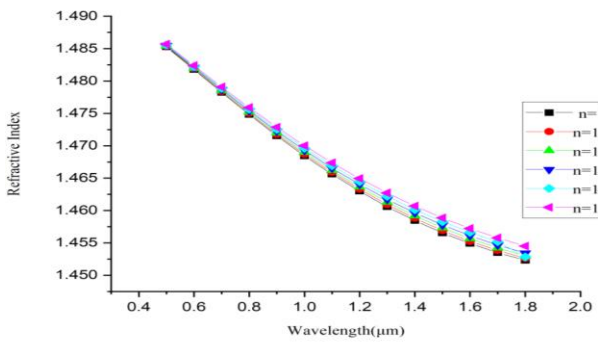

Fig. 2. Plot of wavelength and refractive index distribution of proposed PCF (color online)

3. Numerical analysis and observations

This section basically describes the analysis of sensor on the basis of result obtained for different parameters. The essential sensing parameters such as confinement loss, wavelength sensitivity, resolution, amplitude sensitivity, birefringes and coupling length were numerically analyzed. Finite Difference Domain based simulation tool was used due to the high accuracy of results and less simulation time.

In the first phase we numerically simulated the design to investigate the relationship between refractive index and wavelength under observation. A specific well investigated set of refractive index representing different analytes was selected for the simulation purpose. The design was numerically simulated for each refractive index for a suitable wavelength range spanning till 2 nm. For sensing purpose we required a very small amount of analyte. Femto-second laser-based method or focused ion-beam micromachining method can be employed for PCF-SPR sensor structures which require selective infiltration of the analyte. In the proposed manuscript, we take the range of analyte from 1.34 to 1.39 with 0.01 per unit difference. In this span we can sensed propane, propylene, fresh milk, Trichlorofluoromethane refrigerant gas, Ether, Acetone, Alcohol, acetic acid etc. [33-34]. The different analytes in the group depicted the identical profile, as inferred from the graph in Fig. 2; all the analytes depicted a decreased profile in refractive index values at the higher wavelengths.

In reference to calculate the sensitivity which relates to confinement loss, we firstly investigated the loss, using the imaginary part of refractive index. The expression below depicts the relation of loss with the refractive index [1]:

$$L = 8.686 * \frac{2\pi}{\lambda} * \mathrm{I_m}\,(\mathrm{n_{eff}}) * 10^4 \qquad (2)$$

PCF based SPR sensor operations are based on evanescent field. Since the optical materials are absorbing medium so a complex refractive index is described, where imaginary part of a complex refractive index is the index of absorption [35-36].

Ensuing simulation results of the confinement loss for values of analyte is portrayed in the Fig. 3. It was observed that the confinement loss linearly depends on the refractive index of the analyte. The analyte with refractive index 1.34 predicted the minimal loss of 16.368 db/m as per the records at the wavelength 0.5 µm. The peak value of confinement loss of plasmonic based refractive index sensor as observed from the simulation was 175.7421 db/m at λ = 1.4 µm, analyte measuring refractive index 1.39.

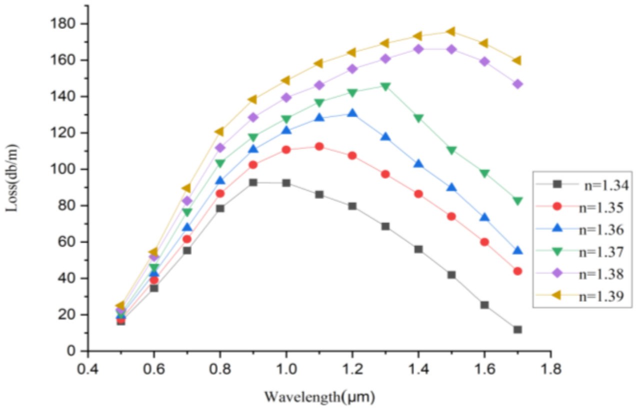

Fig. 3. Confinement loss of proposed PCF sensor for different values of analyte with toluene (color online)

The next vital parameter, which was simulated for the investigation was sensitivity of the sensor. Sensitivity is the most essential parameter for any sensing device, the sensitivity of optical sensors is associated with confinement loss with the change in the analyte. Sensitivity measures rate of change of wavelength per unit change of refractive index of the material under investigation [37]. It is desirable to have a senor with the higher sensitivity. Subsequently the sensitivity was calculated using the underlined expression,

$$S = \Delta\lambda/\Delta n_a \qquad (3)$$

In the expression above, $\Delta\lambda$ is the resonant maximum wavelength shift and Δn_a is analyte refractive index variation. It was inferred from the graph in the Fig. 2, the loss increased for the increasing values of analyte, and the peak of loss depicted a shift towards the higher wavelength side. The peak value of resonance wavelength shift is obtained at 83.3 µm when the analyte refractive change from 1.33 to 1.39. When analyte refractive index is varied from 1.34 to 1.35, 1.35 to 1.36, 1.36 to 1.37, 1.37 to 1.38, 1.38 to 1.39, the corresponding peak wavelength variations are 19.8 µm, 18.1 µm, 15.3 µm, 12.2 µm and 9.6 µm respectively.

By using Δn_a = 0.01 µm, the wavelength sensitivities obtained are 1980, 1810, 1530, 1220 and 960 nm/RIU respectively. And the average wavelength sensitivity is 1500 nm/RIU can be enhanced when RI changes from 1.33 to 1.39 respectively.

Sensor Resolution is also important factor for describing the characteristics of RI based sensor and it can be defined as:

$$\mathrm{R(RIU)} = \Delta n_a \frac{\Delta\lambda_{min}}{\Delta\lambda_{peak}} \qquad (4)$$

Here $\Delta\lambda_{peak}$- shows the resonant peak shift and Δn_a denotes the variation in the refractive index of analyte.

For an evaluation of sensor quality, a small value of resolution is desired to detect small variation in the analyte refractive index from 1.34 to 1.35, 1.35 to 1.36, 1.36 to 1.37, 1.37 to 1.38 and 1.38 to 1.39. When refractive index of analyte is 1.39, we obtained highest sensor resolution is 10.916×10^{-5} RIU. Using $\Delta n_a = 0.01$ and $\Delta\lambda = 0.1$ µm when the analyte refractive index is varied from 1.34 to 1.35, 1.35 to 1.36, 1.36 to 1.37, 1.37 to 1.38 and 1.38 to 1.39, the corresponding value of sensor resolution are 5.05×10^{-5}, 5.52×10^{-5}, 6.535×10^{-5}, 8.196×10^{-5}, 10.416×10^{-5} RIU respectively. It should be noted that when we calculate the sensor resolution, we assumed that the noise influence has no effect on the sensor parameter.

Next, we calculate the amplitude sensitivity. To calculate sensitivity amplitude interrogation method is comparatively simple as compared to wavelength interrogation method [21]. The amplitude sensitivity of the sensor can be defined as:

$$S_A\,(\mathrm{RIU^{-1}}) = -\frac{1}{\alpha(\lambda, n_a)} \frac{\partial\alpha(\lambda, n_a)}{\partial n_a} \qquad (5)$$

where $\partial\alpha$ (λ,n_a) denotes the loss gap due to adjacent analyte RI in terms of wavelength. When RI of analyte is 1.39, the maximum sensor amplitude sensitivity is obtained as 952.381 × 10^{-5} RIU.

Birefringes represented the difference between the two fundamental modes [38, 39]. This can be represented by Equation (6):

$$B = |n_{eff}^{x} - n_{eff}^{y}| \quad (6)$$

where n_{eff}^{x} and n_{eff}^{y} denotes real value of effective refractive index of x and y modes respectively. Due to high birefringes effect, x polarized transverse electric mode (TE) mode shows the larger evanescent field resulting in a stronger coupling with analyte compared to the y polarized TE mode. So when asymmetry is created, then there is a large interaction possibility of light with analyte. It supports the large wavelength shifting, hence increase the sensitivity of plasmonics based refractive index sensor. So these higher birefrigent PCF based sensor can be used as a sensing probe, polarization maintaining device, filtering etc. [40-41].

The maximum value of birefringes is 0.00075735 at wavelength 1.2 μm for the analyte RI n=1.34.

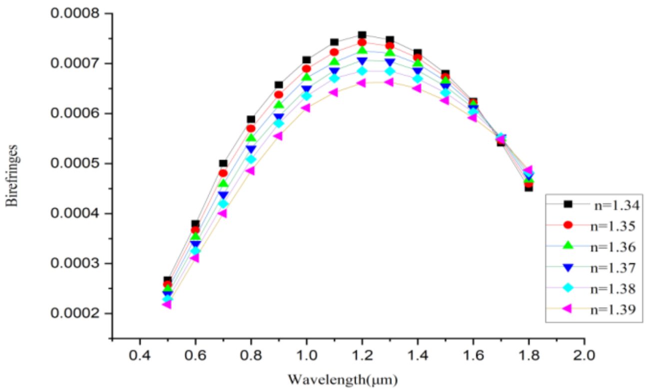

Fig. 4. Birefringes of proposed PCF for different values of analyte (color online)

Birefringes property is generated in the PCF due to asymmetry around the core of the PCF [41]. In our proposed design, asymmetry is generated when there are only eight air holes exists in the second ring and the size of air hole of first and second ring is different. Fig. 4 shows as the wavelength increases, the birefringes also increases. This is due to the difference between real part of n_{eff}^{x} and n_{eff}^{y} increases continuously with wavelength.

The coupling length is the unique parameter to describe the coupling efficiency of concentric core PCF. The minimum coupling length characterizes the strong coupling strength of the fiber [42]. The coupling length can be defined as:

$$CL = \frac{\lambda}{2(n_{eff}^{x} - n_{eff}^{y})} \quad (7)$$

where λ is the incident light of wavelength. Fig. 5 shows that as the wavelength increases, the coupling length also increases. When the refractive index of analyte varies from 1.34 to 1.39, the coupling length also increases.

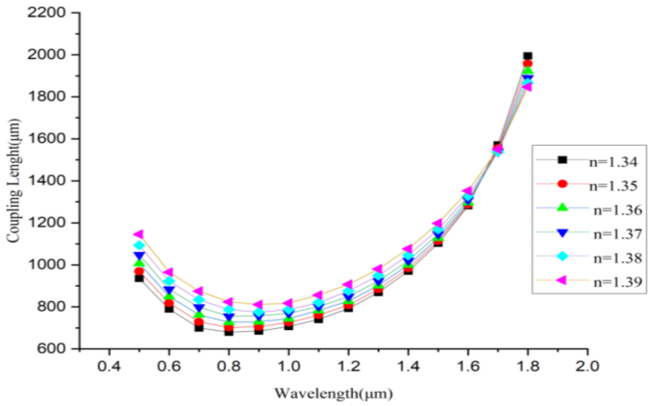

Fig. 5. Coupling length of proposed PCF for six different values of analyte (color online)

Plasmonics have a very remarkable application in plasmonics based refractive index sensor design. The basic principal of plasmonics sensor depends upon the interplay between the metal-dielectric interfaces. When the light incident on the fiber core, then the generated transient field coupled with plasmonic metal layer, generates a surface Plasmon wave. In this sensor, Toluene is used with the gold to increase the SPP interaction to minimize losses and strong confinement. When core guided mode frequency is just equal to the SPP mode, then a sharp peak is obtained in confinement loss graph. Due to small variation in the analyte is directly following the significant change in the sensitivity. Hence, the investigated sensor finds its application as nano dimension sensing.

4. Conclusion

A hybrid profile hexagonal lattice configuration based SPR refractive index sensor is investigated for the analysis of refractive index of analyte. Perfectly matched layer (PML) boundary condition is used on outer most layer of the PCF sensor to absorb the energy of cladding radiation. The proposed sensor exhibits low losses 5.94 db/m at the refractive index 1.37 at the wavelength λ =1.744 μm. As compared to other material, Gold has very large wavelength shifting property as well as chemical stability so gold is most preferred choice for SPR phenomenon. The highest value of birefringes is 0.021401 at λ= 1.9 μm for refractive index 1.35. So the investigated sensor can be used as biological and chemical sensing.

References

[1] Lanh Chu Van, J. Opt. **19**, 125604 (2017).
[2] Yundong Liu, Xili Jing, Shuguang Li, Optics and Laser Technology **114**, 114 (2019).

[3] K. Prabu, R. Malavika, Optical Fiber Technology **47**, 21 (2019).
[4] Yuwei Qu, Jinhui Yuan, Xian Zhou, Feng Li, Optics Communications **452**, 1 (2019).
[5] Liangliang Liu, FengHuan Hao, Stephen P. Morgan, Ricardo Correia, Andrew Norris, Sensing and Bio-Sensing Research **22**, 100254 (2019).
[6] A. Sharafali, K. Nithyanandan, Optik **191**, 121 (2019).
[7] Moutusi De, Vinod Kumar Singh, Photonics and Nanostructures - Fundamentals and Applications **36**, 100722 (2019).
[8] Divya, Selvendran, Raja, Sivasubramanian, Biosensors and Bioelectronics **11**, 100175 (2022).
[9] Azad, Islam, Kaysir Atai, Optik **226**, Part 2, 166009 (2021).
[10] Alexander Kwasi Amoah, Emmanuel Kofi Akowuah, Geoffrey Nukpezah, S. Haxha, Optical Fiber Technology **53**, 102032 (2019).
[11] Fu Qin, Yanhua Dong, Jianxiang Wen, Fufei Pang, Optical Materials **64**, 468473 (2017).
[12] Jianyuan Qin, Bei Zhu, Yong Du, Zhanghua Han, Optical Fiber Technology **52**, 101990 (2019).
[13] Hanrui Yang, Weiliang Huang, Shengxi Jiao, Xiaolong Sun, Wei Hong, Li Qiao, Optik **185**, 390 (2019).
[14] Xingtao Zhao, Qiang Xiong, Guohui Jiang, Lu Hua, Jirui Cheng, Shutao Wang, Optical Fiber Technology **46**, 167 (2018).
[15] Fan Zhenkai, Wang Yingying, Zichao Zhang, Baozhu Wang, Rongjia Zhao, Optical Fiber Technology **49**, 1 (2019).
[16] Yaonan Hou, Journal of Luminescence **208**, 279 (2019).
[17] Moriom Rojy Momota, Md. Rabiul Hasan, Optical Materials **76**, 287 (2018).
[18] Anuj K. Sharma, Ankit Kumar Pandey, Baljinder Kaur, Optical Fiber Technology **43**, 20 (2018).
[19] Zhao Yang, Li Xia, Chen Li, Xin Chen, Optics Communications **430**, 195 (2019).
[20] Nannan Luan, Lei Zhao, Yudong Lian, IEEE Photonics Journal **10**(5), 6806707 (2018).
[21] Nannan Luan, Jianquan Yao, IEEE Photonics Journal **9**(3), 6802107 (2017).
[22] M. Saifur Rahman, Md. Shamim Anower, Labid Bin Bashar, Khaleda Akter Rikta, Sensing and Bio-Sensing Research **16**, 41 (2017).
[23] Sujan Chakma, Md Abdul Khalek, Bikash Kumar Paul, Kawsar Ahmed, Md Rabiul Hasan, Sensing and Bio-Sensing Research **18**, 7 (2018).
[24] Md. Nazmul Hossen, Md. Ferdous, Md. Abdul Khalek, Sujan Chakma, Bikash Kumar Paul, Sensing and Bio-Sensing Research **21**, 1 (2018).
[25] Md. Faizul Huq Arif Mohammad Mobarak Hossain Nazrul Islam, Shah Mostafa Khaled, Sensing and Bio-Sensing Research **22**, 100252 (2019).
[26] Farmani, Homa, Ali Farmani, Zeinab Biglari, Physica E: Low-dimensional Systems and Nanostructures **116**, 113730 (2020).
[28] A. Dixit, S. Tiwari, U. Ramani, P. C. Pandey, Optics & Laser Technology **121**, 105779 (2020).
[29] M. H. Elshorbagy, A. Cuadrado, G. González, F. J. González, J. Alda, Journal of Lightwave Technology **37**(13), 2905 (2019).
[30] B. Ai, C. Song, L. Bradley, Y. Zhao, The Journal of Physical Chemistry C **122**, 20935 (2018).
[31] Sugandha Das, Vinod Kumar Singh Singh, Optik **201**, 163489 (2020).
[32] Araf Shafkat, Mohammad Istiaque Reja, Md. Jalal Miah, Saleha Fatema, Rubaya Absar, Jobaida Akhtar, Optik **231**, 166418 (2021).
[33] Nabarun Polley, Supratim Basak, Roland Hass, Claudia Pacholski, Biosensors and Bioelectronics **132**, 368 (2019).
[34] Shumaia Sharmin, Akash Bosu, Sanjida Akter International Conference on Advancement in Electrical and Electronic Engineering 22-24 November, Gazipur, Bangladesh (2018).
[35] Kawsar Ahmed, Md. Japirul Haque, Md. Aaduzzaman Jabin, Bikash Kumar Paul, Iraj S. Amiri, P. Yupap, Results in Physica B: Condensed Matter. **570**, 48 (2019).
[36] M. S. Aruna Gandhi, K. Sentilnathan, P. Ramesh Babu, Qian Li, Results in Physics **15**, 102590 (2019).
[37] Md. Aslam Mollah, S. M. Abdur Razzak, Alok Kumar Paul, Md. Rabiul Hasan, Sensing and Bio-sensing Research **24**, 100286 (2019).
[38] Sugandha Das, Vinod Kumar Singh, Photonics and Nanostructures- Fundamentals and Applications **44**, 100904 (2021).
[39] Zhenkai Fan, Shuguang Li, Qiang Liu, Guowen An, IEEE Photonics Journal **7**, 4800809 (2015).
[40] Jian Han, Weiquan Su, Chao Liu, Famei Wang, Chunhong Xu, Qiang Liu, Lin Yang, Xianli Li, Tao Sun, Paul K. Chu, Optik **189**, 121 (2019).
[41] Shanshan Zhang, Weiguang Shi, Cheng Zhang, Jia Shi, Jixuan Wu, Hongqiang Li, Yange Liu, Bo Zhang, Optical Materials **79**, 137 (2018).
[42] Junbo Lou, Tonglei Cheng, Shuguang Li, Optical Fiber Technology **48**, 110 (2019).

*Corresponding author: yazushasharma@gmail.com